Title
Intestinal adaptation following spring insertion into a roux limb in mice

Journal
Journal of Pediatric Surgery, 56(2)

ISSN
0022-3468

Authors
Portelli, Katherine I
Park, Jun-Beom
Taylor, Jordan S
et al.

Publication Date
2021-02-01

DOI
10.1016/j.jpedsurg.2020.06.033

Peer reviewed

HHS Public Access

Author manuscript

J Pediatr Surg. Author manuscript; available in PMC 2022 February 01.

Published in final edited form as:

J Pediatr Surg. 2021 February ; 56(2): 346–351. doi:10.1016/j.jpedsurg.2020.06.033.

Intestinal adaptation following spring insertion into a Roux limb in mice

Katherine I. Portelli, MD[a,*], **Jun-Beom Park, MD**[a,*], **Jordan S. Taylor, MD**[a], **Anne-Laure Thomas, MS**[a], **Matthias Stelzner, MD**[b], **Martin G. Martin, MD**[c], **James C.Y. Dunn, MD, PhD**[a,d,†]

[a]Department of Surgery, Stanford University, Stanford, CA

[b]Department of Surgery, University of California, Los Angeles, CA

[c]Department of Pediatrics, University of California, Los Angeles, CA

[d]Division of Bioengineering, Stanford University, Stanford, CA

Abstract

Background/Purpose—Intraluminal springs have recently been shown to lengthen segments of intestine in a process known as distraction enterogenesis. We hypothesized that biocompatible springs could be used to lengthen defunctionalized murine small intestine and would lead to identifiable intestinal adaptations at the molecular level.

Methods—Age and weight matched C57BL/6 mice underwent surgical insertion of nitinol spring-loaded capsules into a Roux limb of jejunum. Segment lengths were measured at initial spring placement and at euthanasia after 14 and 21 days. Histology and gene expression of the Roux limb were evaluated at scarification and compared to untreated control segments.

Results—Intestinal segments loaded with compressed springs lengthened an average of 240%, which was significantly longer than control segments loaded with either empty capsules or uncompressed springs. Muscularis thickening was greater in spring-treated mice compared to controls without springs. Crypt depth and Lgr5+ expression was greater in mice that received compressed spring treatments when compared to control groups.

Conclusions—Insertion of a compressed nitinol spring into a Roux limb results in significant intestinal lengthening, smooth muscle thickening, and Lgr5+ expression in a mouse model. The ability to increase small bowel length in a defunctionalized murine model may be used to understand the mechanism of distraction enterogenesis.

[†]**Correspondence to:** James Dunn, Division of Pediatric Surgery, Stanford University, 300 Pasteur Drive, Alway Building M116, Stanford, CA 94305; Telephone: (650) 723-6439; Fax (650) 725-5577; jdunn2@stanford.edu.

[*]Authors contributed equally this work

Conflicts of Interest: Dr. James C.Y. Dunn is the founder of Eclipse Regenesis, Inc. Remaining authors have no financial relationships relevant to this article to disclose.

Keywords

Short bowel syndrome (SBS); Distraction enterogenesis; Intestinal lengthening; Intestinal failure (IF)

1. INTRODUCTION

Short bowel syndrome (SBS) is a highly morbid condition characterized by inadequate bowel length or capacity to absorb sufficient nutrients or fluids. The most common cause of SBS is bowel resection; however, in children, SBS is often due to congenital anomalies such as atresia, necrotizing enterocolitis, gastroschisis, and volvulus [1]. SBS lacks efficacious and economical treatment options [2,3]. Although comprehensive care teams have been shown to be an important component of survival in patients with SBS [4,5], access to these teams is expensive and highly variable between institutions [2].

Medical management includes combination enteral and parenteral nutrition (PN) to achieve proper caloric intake and optimize electrolyte balance [6]. While the majority of SBS patients can achieve enteral autonomy without surgical intervention, the length of time on PN can lead to psychological and physiological complications. Patients treated with long-term PN experience lower quality of life compared with SBS patients who undergo successful surgical intervention [7]. In addition, longer duration of time on parenteral nutrition is associated with an increased likelihood developing complications such as hepatotoxicity, infection, and device malfunction. These complications often lead to numerous costly hospitalizations [2].

Research has determined residual small bowel length to be the best predictor of PN duration [3,8]. Surgical management with intestinal lengthening procedures such as longitudinal intestinal lengthening and tailoring (LILT) and serial transverse enteroplasty (STEP) procedures have demonstrated a slight reduction in time to enteral autonomy [9,10]. However, these surgical interventions are associated with major complications including obstruction, redialation, perforation, bleeding, abscess, and fistula [11]. Despite exhaustive medical and surgical interventions, progression from SBS to intestinal failure (IF) remains substantial [12].

Distraction enterogenesis techniques using intraluminal springs and hydraulic devices have demonstrated encouraging results in pre-clinical models. Murine and porcine spring studies have demonstrated scalability with consistent small intestinal lengthening and increased epithelial absorptive capacity [13,14,15,16,17]. Endoluminal hydraulic device placement through a jejunal stoma have shown similar degrees of lengthening [18].

While mechanical strain has been substantiated to cause intestinal lengthening and epithelial growth, the underlying molecular mechanisms responsible for these adaptations are not well understood. Here we will determine whether comparable intestinal adaptations occur in a defunctionalized intestinal segment in mice as have previously been demonstrated in larger animal models [14,19,20]. Further, we will investigate the molecular mechanisms responsible for intestinal lengthening and epithelial growth. Utilization of a Roux segment

isolates spring-mediated adaptions and minimizes complication rates, making this model ideal to study the cellular signaling pathways that drive intestinal lengthening, epithelial proliferation, and muscularis augmentation [13,14,15,16]. The aim of this study is to begin preliminary investigations into underlying mechanism involved in intestinal adaptations of spring-mediated distraction enterogenesis and validate our murine Roux model for future in-depth study.

2. MATERIAL AND METHODS

2.1. Spring Design and Preparation

Springs were formed by shape setting heat treatment using a nitinol filament wrapped around a coiled mold as previously described by *Huynh et al* [17]. Uncompressed and compressed spring lengths were measured and spring constants (k) were calculated using a scale and suspension system in accordance with Hooke's law, $F=-kx$, where k = spring constant (N/m), F = force (N), and x = displacement (m). Springs were inserted into 0.025 mL hard gelatin capsules (size 9, Torpac Inc., Fairfield, NJ). Capsules were coated with three layers of cellulose acetate phthalate in acetone to prevent premature spring deployment in vivo. Capsules were sterilized under UV light for 12–24 hours preoperatively.

2.2. Animals and Surgical Procedures

All animal procedures were reviewed and approved by Stanford University's Institutional Care and Use Committee (Protocol # 32497). Twenty-one age and weight matched C57BL/6 mice (Jackson Laboratory, Sacramento, CA) underwent surgical creation of a blind-ending Roux-en-Y jejunojejunostomy as previously described [14,19,20]. In brief, animals were anesthetized with inhaled isoflurane and a ventral midline incision was made to expose the small intestine. The bowel was transected in the mid-jejunum and the distal segment was sutured to form a 1.5 cm defunctionalized Roux limb.

Capsules containing compressed (CS) nitinol springs were inserted into the Roux limb. Empty capsules (EC) and uncompressed springs (US) were inserted into control animals (Figure 1A). Capsules were maintained in position by two plication sutures that decreased the luminal diameter by approximately 50% (Figure 1B). Bowel continuity was restored with anastomosis of the proximal transection site and the distal enterotomy site (Figure 1B). Initial length of the small bowel segment containing the capsule was measured between the blind end and first plication suture.

Animals were initially maintained on a liquid diet and advanced to regular diet on postoperative day (POD) seven. Animals were euthanized on POD14 or POD21 and final intestinal segment length was measured. Treated Roux segments and control segments (10 mm distal to the capsule site) of small bowel were obtained for histology, immunohistochemistry, and RT-PCR.

2.3. Tissue Processing, Histology, and Immunostaining

Retrieved bowel segments were divided and either frozen fresh or fixed in 10% buffered formalin and paraffin embedded. Embedded tissue was sectioned, stained with hematoxylin

and eosin (H&E) and analyzed for villus height, crypt depth, and smooth muscle thickness. Immunofluorescence staining for olfactomedin 4 (Olfm4) and myosin-heavy chain 11 (Myh11) was performed to evaluate changes in crypt cell density and smooth muscle cell proliferation, respectively. Samples were permeabilized by 0.5% Triton-X for 5 minutes and blocked with 2% bovine serum albumin and 4% normal goat serum in 0.05% Tween phosphate-buffered saline at room temperature. Primary antibodies anti-Olfm4 (Cell Signaling Technology, Boston, MA) and anti-Myh11 (Abcam, Cambridge, UK) were incubated overnight at 4 °C. Secondary antibodies (Invitrogen, Carlsbad, CA) were applied at room temperature. Slides were mounted with DAPI (Invitrogen, Carlsbad, CA) and fixed with a coverslip before imaging with an IX73 microscope and cellSense software (Olympus, Tokyo, Japan).

2.4. Quantitative RT-PCR

RT-PCR samples were collected for seven mice in the compressed spring experimental group. G-protein-coupled receptor 5 (Lgr5+) and myosin heavy chain 11 (Myh11) were used as markers for crypt cells and smooth muscle cells, respectively.

Total RNA was extracted from small bowel samples using the RNeasy Mini Kit (Qiagen, Hilden, Germany) following to the protocol provided from Qiagen. The ABI Prism 7900 Sequence Detection System (Applied Biosystems, Carlsbad, CA) and the PCR master mix from Quantitect Probe RT-PCR kit (Qiagen) were used to perform the real time RT-PCR reactions.

PCR primers and probes for amplification of glyceraldehyde 3-phosphate dehydrogenase (Gapdh, Mm99999915_g1), G-protein-coupled receptor 5 (Lgr5 Mm00438890_m1), myosin-heavy chain 11 (Myh11, Mm00443013_m1) were purchased from Taqman (Life Technologies, Carlsbad, CA) and were used according to the protocol provided by the vendor at one times the final concentration in the PCR mix. The Gapdh housekeeping gene was used as a calibrator of gene expression. Cycle threshold numbers were normalized by pooled normal skin set to one for comparison.

2.5. Statistics

Data were reported as mean ± standard deviation (SD). Data analysis, including one-way analysis of variance (ANOVA), post-hoc Tukey Test, and Student’s t-Test, was performed using GraphPad Prism 8 software (GraphPad Software, San Diego, CA). ANOVA with post-hoc Tukey Test analyses were used to compare the average change in small bowel segment lengths between each of the four groups including empty capsule control (EC), uncompressed spring control (US), and compressed spring treatment (CS14 and CS21) groups. Two-tailed paired Student’s t-Test were used to compare PCR results.

3. RESULTS

3.1. Mouse and Spring Characteristics

Nitinol springs had an average uncompressed length of 10±0.5 mm that compressed down to 4.0 mm within the capsules. Spring constants (k) were measured to be 0.77±0.1 N/m. Within

the CS group, there was no significant difference in initial spring length or spring constant (p=0.06 and p=0.96, respectively). There was no significant difference between preoperative and postoperative animal weights across treatment groups (p=0.44 and p=0.80, respectively) (Table 1).

3.2. Intestinal Lengthening

The initial Roux segment length in the control (EC and US), CS14, and CS21 groups was 4.4±0.2 mm, 4.3±0.3 mm, and 4.3±0.3 mm respectively (p=0.60). Intestinal segments loaded with compressed springs lengthened an average of 6.0±0.7 mm compared to control segments which lengthened an average of 0.80±0.7 mm (p<0.0001). The final average length of compressed spring-treated segments was 10.2±0.5 mm or 240±0.2% of the average initial segment lengths while the final average length of control segments (EC and US) was 5.2±0.8 mm or 120±0.2% of initial segment lengths (p<0.0001) (Table 2).

3.3. Histology and Immunofluorescence

Smooth muscle thickness of the control (EC and US), CS14, and CS21 groups was 52±26 μm, 64±41 μm, and 72±25 μm respectively (p=0.27). Smooth muscle thickness was greater in CS groups on both POD14 (120±71 μm) and POD21 (250±110 μm) when compared to control bowel segments (p=0.0037 and p<0.0001, respectively). Smooth muscle thickening in the CS mice on POD21 (178±110 μm, p<0.001) was greater than CS mice at POD14 (56±58 μm) and control (EC and US) mice (14±55 μm) (p=0.0008 and p<0.0001, respectively) (Table 3). Gross histologic evaluation demonstrated greater disorganization of the smooth muscle in capsule-treated segments compared to respective controls (Figure 2).

Control segment crypt depth was similar in all groups with an average depth of 87±20 μm (p=0.50). Crypt cells had greater depth in CS segments at POD21 (140±30 μm) compared to both CS segments at POD14 (91±28 μm) and control (EC and US) segments (72±39 μm) (p=0.0022 and p=0.0487, respectively). Crypt depth was greater in CS groups on POD21 (140±30 μm) compared to respective control segments (p=0.0167). Crypt depth increased by an average of 46±26 μm in CS segments at POD21 while crypt depth decreased by an average of 16±54 μm in control (EC and US) segments (p=0.0321) (Table 4). There was no difference in villi height between treatment and control segments (p=0.52) (Table 5).

Olfm4 signals demonstrated increased height and density in CS treated segments compared control segments at POD21. Myh11 fluorescent signaling demonstrated greater width in CS treated segments at both POD14 and POD21 when compared to respective control segments (Figure 3).

1.3.3 Quantitative RT-PCR—RT-PCR demonstrated 4.3±2.6 times higher Lgr5+ expression in CS spring-treated bowel segments compared with normal bowel control segments at POD21 (p=0.047) (Figure 4A). There was no difference in Myh11 expression in either CS spring-treated groups compared to control at either POD14 or POD21 (p= 0.33 and p=0.061, respectively) (Figure 4B).

4. DISCUSSION

Distraction enterogenesis is emerging as a promising method for inducing intestinal lengthening in the treatment of short bowel syndrome. Previous work has demonstrated significant lengthening can be achieved in pre-clinical, large animal models using intraluminal springs within in-continuity intestine [15,16]. Lengthening of Roux limb intestine has also been previously demonstrated in large animal and rodent models [14,19,20]. In this work, we aimed to develop a feasible murine model of intestinal lengthening in order to study the underlying mechanisms of distraction enterogenesis. We established a Roux limb model that induces significant lengthening comparable to previous work and began studies into potential underlying mechanisms.

Regarding the gross and histologic changes induced by an intraluminal spring in our model, there was significant lengthening of Roux limb segments when a compressed spring was implanted compared to empty capsule or uncompressed spring controls. The spring force also increased crypt depth by POD21 and thickened murine smooth muscle by POD14. While the organizational structure of the smooth muscle layer was not formally evaluated during this study, we perceived greater gross disorganization of the smooth muscle layer in capsule-treated segments compared to respective control segments. This observed disorganization could be the result of smooth muscle restructuring or human error in sample processing and requires further study.

This model can be utilized in future research to investigate the mechanisms behind successful lengthening. In these experiments, we evaluated Olfm4 expression using immunohistochemistry and found an increased height and density of Olfm4 signaling in the compressed spring group at POD21, indicative of crypt cell proliferation and increased crypt cell density. The crypt cell proliferation was correlated with a similar elevation in Lgr5+ expression seen in RT-PCR. The spring force leads to an increase in crypt cell density and proliferation, which could increase the nutrient absorption and support growth. We hypothesize that this proliferation drives an increase in functional capacity of the CS treated segment; however, more work is needed to verify these crypts contribute to increased functional absorptive capacity.

On immunofluorescence, there was an increased width of the Myh11 signaling band in the CS groups; however, mRNA expression was not significantly different between the groups at either POD14 or POD21. The changes in Myh11 protein expression may be related to post-transcriptional changes of the smooth muscle. More work is needed to determine how and by what mechanism the smooth muscle is affected by spring force.

This study has several limitations, most notably in the sample size possibly contributing to a type II error. This work was intended to establish a reliable model for assessing the mechanisms behind spring-mediated lengthening, the timing of which is still under investigation. Future work may need to examine the effects of the spring at different time points to completely understand the factors involved with growth. In addition to studying the mechanisms of epithelial proliferation and muscle adaptations seen in this model, future work will focus on re-establishing the lengthened segment back into continuity and

observing long-term intestinal changes. Future studies will also need to evaluate these spring-mediated adaptations in-continuity in order to elucidate results with more clinical utility to patients with short bowel syndrome.

5. CONCLUSIONS

Insertion of a compressed nitinol spring into a defunctionalized Roux limb results in significant intestinal lengthening, crypt cell proliferation, and smooth muscle hypertrophy. This model replicates the lengthening seen in other pre-clinical models of spring-mediated distraction enterogenesis and provides initial insight into the underlying molecular mechanisms responsible for intestinal adaptation due to spring force. Further studies will explore these underlying pathways in greater depth and will investigate mechanisms of spring-mediated intestinal adaptations in-continuity.

ACKNOWLEDGEMENTS

Supported by an NIH award U01DK085535 (Intestinal Stem Cell Consortium of the NIDDK and NIAID).

Funding Source: This research was supported by the National Institutes of Health [grant number U01DK085535] (Intestinal Stem Cell Consortium of the NIDDK and NIAID).

Abbreviations

SBS	short bowel syndrome
IF	intestinal failure
PN	parenteral nutrition
TPN	total parenteral nutrition
LILT	longitudinal intestinal lengthening and tailoring
STEP	serial transverse enteroplasty
Olfm4	olfactomedin 4
Myh11	myosin heavy chain 11
Lgr5+	leucine-rich repeat-containing G-protein coupled recept
H&E	hematoxylin and eosin
Gapdh	glyceraldehyde 3-phosphate dehydrogenase
DAPI	4’,6-diamidino-2-phenylinodole
ANOVA	analysis of variance
CS	compressed spring
US	uncompressed spring
EC	empty capsule

POD	post-operative day

7. REFERENCES

1. Buchman AL. Etiology and Initial Management of Short Bowel Syndrome. Gastroenterology. 2006;130(2):S5–S15. [PubMed: 16473072]
2. Spencer AU, Kovacevich D, McKinney-Barnett M, et al. Pediatric short-bowel syndrome: the cost of comprehensive care. Am J Clin Nutr. 2008;88(6):1552–1559. [PubMed: 19064515]
3. Fallon EM, Mitchell PD, Nehra D, et al. Neonates With Short Bowel Syndrome. JAMA Surg. 2014;149(7):663. [PubMed: 24827450]
4. Hess RA, Welch KB, Brown PI, Teitelbaum DH. Survival Outcomes of Pediatric Intestinal Failure Patients: Analysis of Factors Contributing to Improved Survival Over the Past Two Decades. J Surg Res. 2011;170(1):27–31. [PubMed: 21601876]
5. Modi BP, Langer M, Ching YA, et al. Improved survival in a multidisciplinary short bowel syndrome program. J Pediatr Surg. 2008;43(1):20–24. [PubMed: 18206449]
6. Sigalet D, Boctor D, Robertson M, et al. Improved Outcomes in Paediatric Intestinal Failure with Aggressive Prevention of Liver Disease. Eur J Pediatr Surg. 2009;19(06):348–353. [PubMed: 19866409]
7. Avitzur Y, Miserachs M. Quality of life on long-term parenteral nutrition. Curr Opin Organ Transplant. 1 2018:1. [PubMed: 29210727]
8. Andorsky DJ, Lund DP, Lillehei CW, et al. Nutritional and other postoperative management of neonates with short bowel syndrome correlates with clinical outcomes. J Pediatr. 2001;139(1):27–33. [PubMed: 11445790]
9. Buchman AL, Moukarzel AA, Bhuta M, et al. Parenteral Nutrition Is Associated With Intestinal Morphologic and Functional Changes in Humans. Vol 19; 1995.
10. Javid PJ, Kim HB, Duggan CP, Jaksic T. Serial transverse enteroplasty is associated with successful short-term outcomes in infants with short bowel syndrome. J Pediatr Surg. 2005;40(6):1019–1024. [PubMed: 15991189]
11. King B, Carlson Gordon, Khalil BA, Morabito A. Intestinal Bowel Lengthening in Children with Short Bowel Syndrome: Systematic Review of the Bianchi and STEP Procedures.
12. Brown SK, Davies N, Smyth E, et al. Intestinal failure: the evolving demographic and patient outcomes on home parenteral nutrition. Acta Paediatr. 2018;107(12):2207–2211. [PubMed: 29754463]
13. Huynh N, Dubrovsky G, Rouch JD, et al. Three-dimensionally printed surface features to anchor endoluminal spring for distraction enterogenesis. PLoS One. 2018;13(7):e0200529. [PubMed: 30001433]
14. Rouch JD, Huynh N, Scott A, et al. Scalability of an endoluminal spring for distraction enterogenesis. J Pediatr Surg. 2016;51:1988–1992 [PubMed: 27665493]
15. Dubrovsky G, Huynh N, Thomas A-L, Shekherdimian S, Dunn JC. Double plication for spring-mediated in-continuity intestinal lengthening in a porcine model. Surgery. 9 2018.
16. Huynh N, Rouch JD, Scott A, et al. Spring-mediated distraction enterogenesis in-continuity. 2016.
17. Huynh N, Dubrovsky G, Rouch JD, et al. Feasibility and scalability of spring parameters in distraction enterogenesis in a murine model. J Surg Res. 2017;215:219–224. [PubMed: 28688651]
18. Demehri FR, Utter B, Freeman JJ, et al. Development of an endoluminal intestinal attachment for a clinically applicable distraction enterogenesis device. J Pediatr Surg. 2016;51(1):101–106. [PubMed: 26552895]
19. Scott A, Sullins VF, Steinberger D, et al. Repeated Mechanical Lengthening of Intestinal Segments in a Novel Model. J Pediatr Surg. 2015;50(6):954–957. [PubMed: 25818320]
20. Sullins VF, Scott A, Wagner JP, et al. Intestinal lengthening in an innovative rodent surgical model. J Pediatr Surg. 2014;49(12):1791–1794. [PubMed: 25487485]

HIGHLIGHTS

- Biocompatible springs can be used to lengthen defunctionalized murine small intestine
- Spring force leads to crypt cell proliferation and increased crypt cell density
- Immunohistochemical evaluations of intestinal smooth muscle reveal an increased width of the Myh11 signaling band, indicating smooth muscle hypertrophy

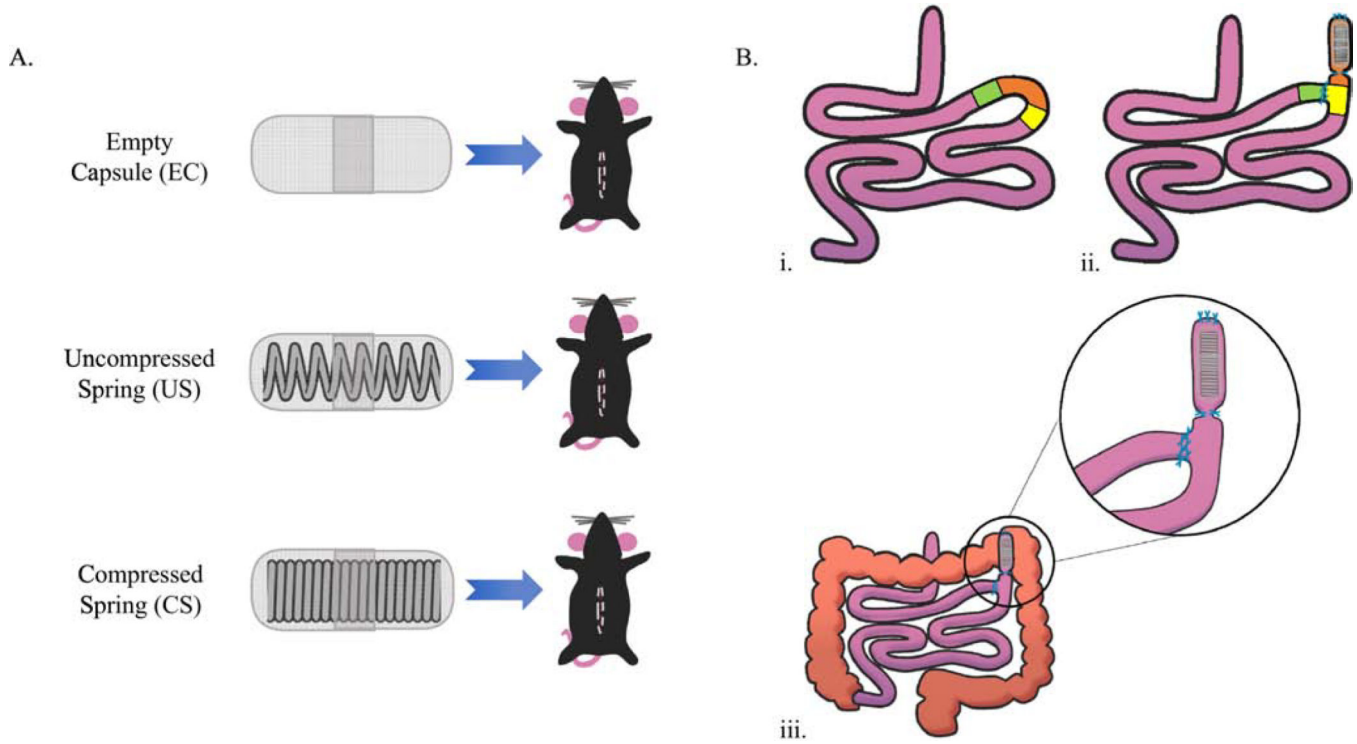

Figure 1.

(A) Experimental Design. Empty capsule group and uncompressed spring group as controls. EC (n=2), US (n=3), CS (n=16). *EC = empty capsule, US = uncompressed spring, CS = compressed spring.* (B) i. Preoperative model of the small bowel. Green: Proximal transection site; Orange: Distal transection site; Yellow: Transverse enterotomy site. ii. Postoperative model of the small bowel, defunctionalized Roux limb, and encapsulated spring. Green: Proximal anastomosis site; Orange: Roux limb; Yellow: Distal anastomosis site. iii. Model of postoperative small bowel.

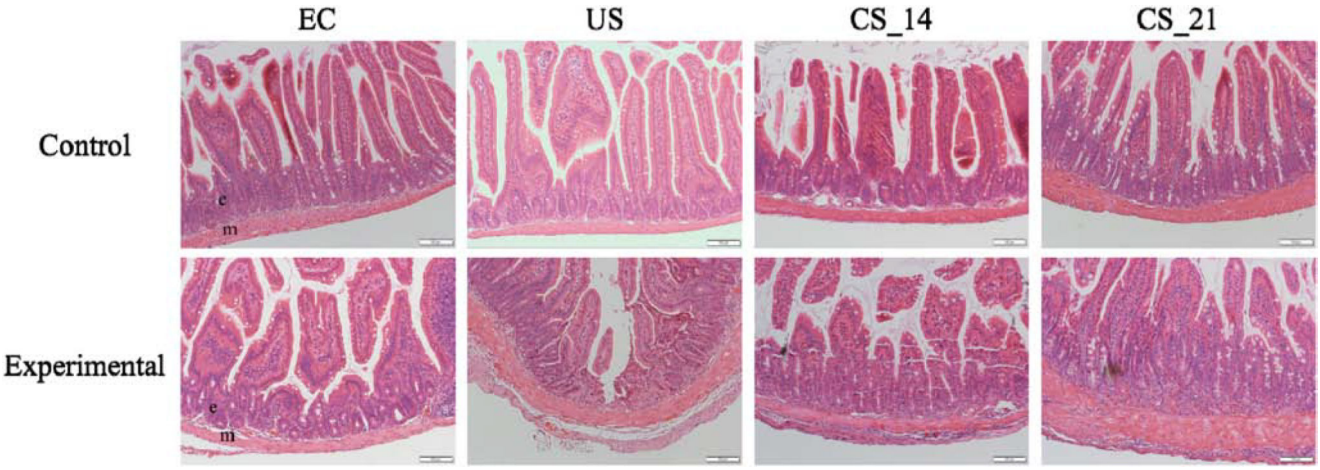

Figure 2.

Histopathology. Comparison of changes in smooth muscle thickness, crypt depth, and villi height between control and experimental segments in empty capsule, uncompressed spring, and spring-treated groups. *EC = empty capsule, US = uncompressed spring, CS POD14 = compressed spring, day 14 scarification, CS POD21 = compressed spring, day 21 scarification.* (Magnification: 100μm)

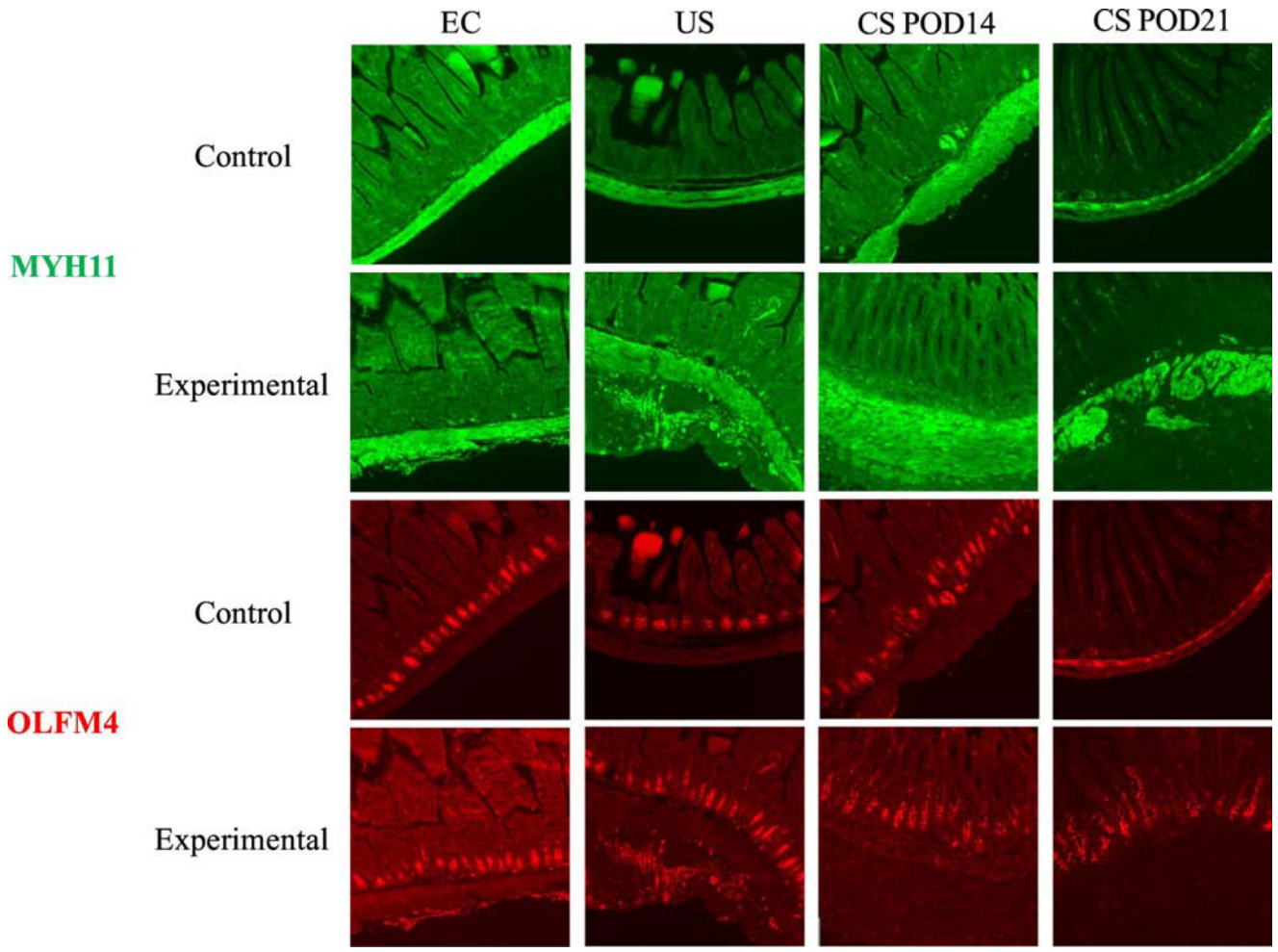

Figure 3.

Immunofluorescence images of spring-treated and control small intestinal segments expressing Myh11 (green), Olfm4 (red), and merged Myh11, Olfm4, and DAPI (blue). Increased width of Myh11 signaling band in CS14 and CS21 spring-treated intestinal segments compared to respective control segments. Increased height and density of Olfm4 signaling in CS21 spring-treated bowel segments compared to control segment. *Myh11 = myosin heavy chain 11, Olfm4 = olfactomedin-4, DAPI = 4′,6-diamidino-2-phenylindole, EC = empty capsule, US = uncompressed spring, CS POD14 = compressed spring, day 14 scarification, CS POD21 = compressed spring, day 21 scarification.* (Magnification: 100μm)

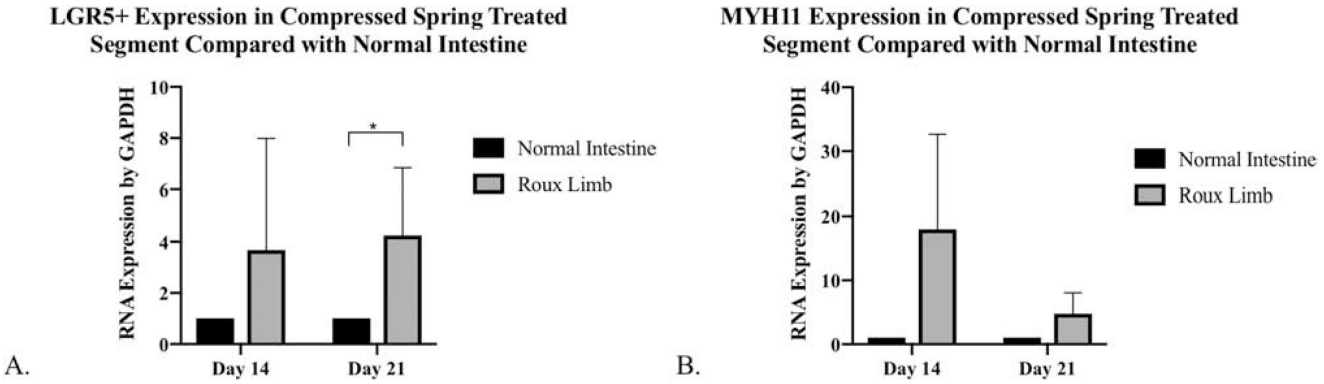

Figure 4.

Level of mRNA expression. Comparison of Lgr5+ (A) and Myh11 (B) expression in CS treated experimental segment vs. control segment at POD7. Student's t-Test analysis shows significant increase in Lgr5+ expression in compressed spring treatment group at POD21 compared to control. Asterisk (*) indicates $p<0.05$.

Table 1.

Baseline mouse characteristics including weight and initial Roux segment length. Spring parameters included spring constant (k) and initial spring length for CS group prior to encapsulation. No significant difference in mouse or spring characteristics. *Control = empty capsule and uncompressed spring, CS_14 = compressed spring, day 14 scarification, CS_21 = compressed spring, day 21 scarification.*

Baseline mouse and spring characteristics					
Values displayed as mean ± SD		**Control**	**CS_14**	**CS_21**	
Mouse					
	initial weight (g)	23±1.9	24±3.9	24±0.6	p = 0.44
	final weight (g)	23±2.4	24±3.9	22±0.5	p = 0.80
	initial segment length (mm)	4.4±0.2	4.3±0.3	4.3±0.3	p = 0.68
Spring					
	constant (N/m)		0.77±0.1	0.77±0.2	p = 0.96
	spring length (mm)		11±0.5	10±0.0	p = 0.06

Table 2.

Intestinal lengthening by treatment group. One-way ANOVA and Tukey test comparison of initial segment lengths, final segment lengths, the difference between initial and final lengths, and final intestinal lengths as a percent of initial segment lengths. Asterisks (*) indicate p<0.0001. *Control = empty capsule and uncompressed spring, CS_14 = compressed spring, day 14 scarification, CS_21 = compressed spring, day 21 scarification.*

Intestinal Segment				
Values displayed as mean ± SD	**Control**	**CS_14**	**CS_21**	
Initial Length (mm)	4.4±0.2	4.3±0.3	4.3±0.3	p = 0.60
Final Length (mm)	5.2±0.8	10.6±0.5	9.8±0.5	*p < 0.0001
Δ Length (mm)	0.80±0.7	6.3±0.6	5.5±0.7	*p < 0.0001
Percent of Initial Length (%)	120±0.2	250±0.2	230±0.2	*p < 0.0001

Table 3.

Comparison of smooth muscle thickness in normal intestinal segment compared with spring-treated segment. Asterisks (*) indicate p<0.0001. *Control = empty capsule and uncompressed spring, CS_14 = compressed spring, day 14 scarification, CS_21 = compressed spring, day 21 scarification.*

Smooth Muscle Thickness				
Values displayed as mean ± SD	**Control**	**CS_14**	**CS_21**	
Control Segment Thickness (μm)	52±26	64±41	72±25	p=0.27
Experimental Segment Thickness (μm)	66±41	120±71	250±110	*p<0.0001
Δ Thickness (μm)	14±55	56±58	178±110	*p<0.0001

Table 4.

Comparison of crypt depth in normal intestinal segment compared with spring-treated segment. Asterisks (*) indicate p<0.01. *Control = empty capsule and uncompressed spring, CS_14 = compressed spring, day 14 scarification, CS_21 = compressed spring, day 21 scarification.*

Crypt Depth				
Values displayed as mean ± SD	**Control**	**CS_14**	**CS_21**	
Control Segment Depth (μm)	88±17	82±21	94±22	p=0.50
Experimental Segment Depth (μm)	72±39	91±28	140±30	*p=0.003
Δ Depth (μm)	−16±54	9.0±26	46±26	p=0.10

Table 5.

Comparison of villi height in normal intestinal segment compared with spring-treated segment. *Control = empty capsule and uncompressed spring, CS_14 = compressed spring, day 14 scarification, CS_21 = compressed spring, day 21 scarification.*

Villi Height				
Values displayed as mean ± SD	**Control**	**CS_14**	**CS_21**	
Control Segment Height (μm)	280±65	260±69	290±42	p=0.63
Experimental Segment Height (μm)	250±110	240±44	310±24	p=0.12
Δ Height (μm)	−30±110	−20±66	20±60	p=0.52